IEEE Access
Multidisciplinary | Rapid Review | Open Access Journal

Received 14 July 2023, accepted 30 July 2023, date of publication 7 August 2023, date of current version 15 August 2023.

Digital Object Identifier 10.1109/ACCESS.2023.3303107

RESEARCH ARTICLE

Change Detection Method for Wavelength-Resolution SAR Images Based on Bayes' Theorem: An Iterative Approach

DIMAS IRION ALVES[1], (Member, IEEE), BRUNA GREGORY PALM[2], (Member, IEEE), HANS HELLSTEN[3], (Senior Member, IEEE), RENATO MACHADO[1], (Senior Member, IEEE), VIET THUY VU[2], (Senior Member, IEEE), MATS I. PETTERSSON[2], (Senior Member, IEEE), AND PATRIK DAMMERT[4,5], (Senior Member, IEEE)

[1]Department of Telecommunications, Aeronautics Institute of Technology (ITA), São José dos Campos 12228-900, Brazil
[2]Department of Mathematics and Natural Sciences, Blekinge Institute of Technology (BTH), 371 79 Karlskrona, Sweden
[3]School of Information Technology, Halmstad University, 301 18 Halmstad, Sweden
[4]SAAB AB Surveillance, SAAB AB, 412 89 Gothenburg, Sweden
[5]Chalmers University of Technology, 412 96 Gothenburg, Sweden

Corresponding author: Dimas Irion Alves (dimasirion@ita.br)

This work was supported in part by the Coordination for the Improvement of Higher Education Personnel (CAPES), Brazil, under Finance Code 001 (Pró-Defesa IV) and through the Scholarship Grant 88887.474585/2020-00; in part by the Brazilian National Council of Scientific and Technological Development (CNPq) under Grant 200759/2020-5; and in part by the Swedish-Brazilian Research and Innovation Centre (CISB).

ABSTRACT This paper presents an iterative change detection (CD) method based on Bayes' theorem for very high-frequency (VHF) ultra-wideband (UWB) SAR images considering commonly used clutter-plus-noise statistical models. The proposed detection technique uses the information of the detected changes to iteratively update the data and distribution information, obtaining more accurate clutter-plus-noise statistics resulting in false alarm reduction. The Bivariate Rayleigh and Bivariate Gaussian distributions are investigated as candidates to model the clutter-plus-noise, and the Anderson-Darling goodness-of-fit test is used to investigate three scenarios of interest. Different aspects related to the distributions are discussed, the observed mismatches are analyzed, and the impact of the distribution chosen for the proposed iterative change detection method is analyzed. Finally, the proposed iterative method performance is assessed in terms of the probability of detection and false alarm rate and compared with other competitive solutions. The experimental evaluation uses data from real measurements obtained using the CARABAS II SAR system. Results show that the proposed iterative CD algorithm performs better than the other methods.

INDEX TERMS Bayes' theorem, CARABAS II, iterative change detection, SAR, wavelength-resolution SAR images.

I. INTRODUCTION

Synthetic aperture radar (SAR) systems are frequently employed for monitoring and surveillance applications [1], [2], [3] due to their specific characteristics, i.e., imaging capability, the small size of the device's antennas, and spatial resolution. Historically, detecting concealed targets in regions with high-density vegetation has been of great interest among SAR systems applications, especially for military purposes [4]. Systems used in this scenario are known as foliage-penetration (FOPEN) radars. FOPEN applications are not possible when traditional microwave SAR systems are employed. Instead, ultra-high frequency (UHF) and very-high frequency (VHF) ultra-wideband (UWB) SAR systems are preferable to be used in FOPEN applications because of their larger wavelengths, large fractional bandwidth, and wide antenna bandwidth, yielding system resolutions in the order of the radar signal wavelengths. The images obtained by these systems are often called wavelength-resolution SAR images. One example of UWB VHF SAR systems is the

The associate editor coordinating the review of this manuscript and approving it for publication was Gang Mei.

coherent all-radio band sensing (CARABAS) II system [5]. The data set considered in this article can be obtained in [6].

Based on the system design and the backscattering phenomenology characteristics [7], UWB wavelength-resolution SAR images are not very sensitive to small scatterers present in the ground area of interest, i.e., objects with dimensions significantly smaller than the signal wavelength, which reduces the false alarms associated with the forest canopy. Thus, the scattering process is mainly related to scatterers with dimensions in the order of the signal wavelengths. For instance, in FOPEN applications, the foliage backscatter is dominated by the direct and ground-reflected backscattering from the tree stems [8]. Based on the scattering process and the system resolution, there might be only a single scatter in the system resolution cell. Consequently, the images do not suffer from a significant contribution of speckle noise [9]. Also, large scatterers are related to large objects, which are frequently less sensitive to weather conditions and, therefore, more stable in time [9]. Due to time stability, obtaining images with high similarity from multi-pass measurements is possible.

One application of interest for FOPEN scenarios is the detection of targets concealed under the forest canopy [10]. Change detection (CD) is a research topic of interest, and several methods have been proposed for this kind of application [10], [11], [12], [13], [14], [15], [16]. Particularly, VHF wavelength-resolution SAR systems associated with CD techniques can be used to detect concealed targets [10], [13], [14], [15], [16]. The first change detection methods for this type of SAR image were based on space-time adaptive processing (STAP) techniques associated with a likelihood-ratio test (LRT) [10], [16]. These CD methods explored the space-time stability of targets and clutter signals as input in an LRT test to detect targets for a fixed false alarm probability.

The proposed methods in [10] and [16] were part of the motivation for other proposals [17], [18], [19]. For example, in [16], the authors consider the clutter-plus-noise statistical model as Bivariate Gaussian distributed due to its simplicity, even knowing that this choice is not ideal. The authors mentioned that more accurate models could provide better performances, which motivated using the Bivariate Gamma distribution in [18] and both Bivariate Rayleigh and K-distributions in [19]. It is important to highlight that the clutter-plus-noise statistical model of VHF wavelength-resolution SAR images is still under investigation [9], [20], [21].

More recently, new methods were proposed for change detection applied in VHF wavelength-resolution SAR images, such as using Bayes' theorem in change detection implementations [17], [22], [23] and small image stacks as input [20], [24], [25]. These methods achieved very competitive performance compared with traditional STAP-based change detection methods in terms of both detection probability and false alarms [17], [24]. Also, iterative detection techniques were proposed aiming to reduce the false alarm occurrence in the SAR change detection scenarios [26], [27], [28].

Motivated by the performance gains associated with the use of an accurate clutter-plus-noise statistical model [16], the false alarm reduction related to iterative detection techniques [26], [27], [28], and the use of Bayes' theorem in change detection methods [17], [22], [23], this paper proposes an iterative change detection method based on Bayes' theorem for VHF wavelength-resolution SAR images. The proposed technique consists of using Bayes' theorem implementation based on a candidate clutter-plus-noise statistical model, which is iteratively updated after each detection using the information associated with the detected candidate object. Additionally, an investigation of the choice between two models for clutter-plus-noise distribution is presented.

The proposed method is assessed using a data set obtained from real measurements with the CARABAS II SAR system. The experimental results show that the proposed methods have competitive performance when compared with other recently proposed methods. The main contributions of this paper are:

- An investigation of two candidate distributions for the clutter-plus-noise statistical modeling using the goodness-of-fit (GoF) test. The tests are performed in VHF wavelength-resolution SAR images.
- The proposition and evaluation of an iterative change detection method for VHF wavelength-resolution SAR images based on Bayes' theorem.

The rest of this document is organized as follows. Section II presents the use of Bayes' theorem for change detection in SAR images. Section III provides an investigation related to the clutter-plus-noise statistical model for VHF UWB wavelength-resolution SAR images. The proposed iterative change detection method is presented in Section IV. Section V presents the data set used in the experiments, some implementation aspects, and the assessment of the proposed method. The contributions of the paper and the proposed method performance are discussed in Section VI. Finally, some concluding remarks are provided in Section VII.

II. BAYES' THEOREM FOR SAR CHANGE DETECTION

The proposed iterative CD method is based on applying Bayes' theorem into SAR CD, as described in [17], which is a modification of the implementation described in [22] and [23]. This section briefly describes the use of Bayes' theorem in the detection of changes in SAR images. The use of two images characterizes the SAR change detection scenario considered in this paper; one is the surveillance image, i.e., the image where it is expected that the changes occurred, and the other is the reference image, i.e., the image used to aid the detection of the changes in the surveillance image. Based on the implementation presented in [22] and [23], the probability of detecting a change for a

given pixel under evaluation can be expressed by

$$P\left(s \equiv s_T | z_s, z_r\right) = \frac{P\left(z_s | s \equiv s_T, z_r\right) P\left(s \equiv s_T | z_r\right)}{P\left(z_s | z_r\right)}, \quad (1)$$

where z_s and z_r are the complex value associated to the evaluated pixel position s, in the surveillance and reference image, respectively, and $s \equiv s_T$ is the statement that the evaluated image sample contains a change. According to [17], the probability of detecting a change for a given pixel under evaluation can be expressed by

$$P\left(s \equiv s_T | z_s, z_r\right) = 1 - \frac{P\left(z_s, z_r | s \not\equiv s_T\right)}{P\left(z_s, z_r\right)} \left[1 - \frac{VK}{N}\right], \quad (2)$$

where V is the number of samples that are expected for a change to occupy, K is the number of detected changes, N is the number of image samples, and $s \not\equiv s_T$ is the statement that the evaluated sample does not contain a change. The probability $P\left(z_s, z_r | s \not\equiv s_T\right)$ can be obtained by using an adequate clutter-plus-noise statistical model, while the joint probability $P\left(z_s, z_r\right)$ can be obtained from the data histogram. The selection of the parameters is related to the application and is discussed on the next sections.

For an adequate choice of the statistical model in (2), the presence of a change in a sample tend to result in $P\left(z_s, z_r\right) \gg P\left(z_s, z_r | s \not\equiv s_T\right)$, leading to $P\left(s \equiv s_T | z_s, z_r\right) \approx 1$. Similarly, in case of the absence of changes results in $P\left(z_s, z_r\right) \approx P\left(z_s, z_r | s \not\equiv s_T\right)$, making $P\left(s \equiv s_T | z_s, zr\right) \approx 0$. However, if the choice of the model in (2) is inadequate, the mismatch between the selected distribution and the data could result in values below 0. Since the method is proposed to detect changes, the inconsistency mentioned above can be overcome by rewriting (2) as

$$P\left(s \equiv s_T | z_s, z_r\right) = \max\left(0,\ 1 - \frac{P\left(z_s, z_r | s \not\equiv s_T\right)}{P\left(z_s, z_r\right)} \times \left[1 - \frac{VK}{N}\right]\right). \quad (3)$$

Unlike [22], [23], where the study focuses on a target geometry analysis, this paper focuses on using the clutter-plus-noise statistical model to enhance the capability of the CD method to reduce false alarms. The current analysis differs from [17] by avoiding $P\left(s \equiv s_T\right) = 0$ and exploring the method iteratively. Additionally, due to the characteristics of the evaluated data set presented in Section V-A, we limit our method evaluation to an incoherent SAR change detection scenario where z_s and z_r represent the pixel magnitude under evaluation.

III. BACKGROUND STATISTICS ANALYSIS

As observed in Section II, the adequate selection of the statistical model for the clutter-plus-noise is necessary to estimate the probability $P\left(z_s, z_r | s \not\equiv s_T\right)$ accordingly. Among the distribution candidates for modeling the clutter-plus-noise in VHF wavelength-resolution SAR images, the Bivariate Rayleigh distribution is seen as the simplest one since it belongs to a one-parameter family of probability distributions. Due to its simplicity, this distribution was selected to evaluate the non-iterative change detection method proposed in [17]. Also, the distribution was already used in other change detection methods [19], [29], presenting a good performance for this type of image. The Bivariate Rayleigh probability density function (pdf) can be written as [30]

$$p\left(z_s, z_r\right) = \frac{4 z_r z_s}{\Omega_r \Omega_s \left(1-\rho\right)} \times \exp\left\{-\frac{1}{1-\rho}\left(\frac{z_r^2}{\Omega_r} + \frac{z_s^2}{\Omega_s}\right)\right\} \times I_0\left(\frac{2\sqrt{\rho}}{1-\rho}\frac{z_r z_s}{\sqrt{\Omega_r \Omega_s}}\right), \quad (4)$$

where $\Omega_r = \overline{z_r^2}$, $\Omega_s = \overline{z_s^2}$, $I_0\left(c\right)$ is the modified Bessel function of the first kind with order zero, and ρ is the correlation coefficient, which can be estimated by [30]

$$\rho = \frac{\mathrm{cov}(z_s^2, z_r^2)}{\sqrt{\mathrm{var}(z_s^2)\mathrm{var}(z_r^2)}}. \quad (5)$$

As previously mentioned, the probabilities $P\left(z_s, z_r | s \not\equiv s_T\right)$ and $P\left(z_s, z_r\right)$ are obtained, respectively, from the selected clutter-plus-noise distribution model and from the data histogram. Figure 1 compares the theoretical Bivariate Rayleigh surface plot obtained from (4) and (5) and the three-dimensional histogram obtained from the experimental data from two evaluated data set image samples. As can be observed, there is a mismatch between the selected Bivariate Rayleigh distribution and the three-dimensional data histogram. For low amplitudes values of z_s and z_r, a possible candidate target pattern is observed, since $P\left(z_s, z_r\right) > P\left(z_s, z_r | s \not\equiv s_T\right)$. However, generally in change detection applications, this observed pattern is not expected, which may contribute to increase the number of false alarms. Another pattern is observed in the theoretical distribution curve decay, where $P\left(z_s, z_r\right) < P\left(z_s, z_r | s \not\equiv s_T\right)$. This observed pattern results in the same situation as observed in (2) and treated in (3), i.e., the impossibility of detecting any target for this range of amplitude values. Given the nature of the surface plot, it is not simple to observe other mismatch patterns in Figure 1.

To further discuss the choice for the clutter-plus-noise distribution model, we evaluate the mismatch between the data histogram and theoretical distribution for a single SAR image. Under the same assumption and considerations of [19], we extrapolate the analysis for the joint probabilities to a single image analysis based on its probability density function. Thus, the surveillance image is modeled as Rayleigh distributed for this analysis. The shape parameter of the theoretical Rayleigh distribution was obtained using a maximum likelihood estimator (MLE). Figure 2 shows the theoretical Rayleigh distribution and the histogram of the experimental data.

As expected, the patterns observed in Figure 1 are also visible in Figure 2. Additionally, we can observe that the majority of the mismatches are present in regions with low amplitude values, i.e., $z_s < 0.4$. Based on this

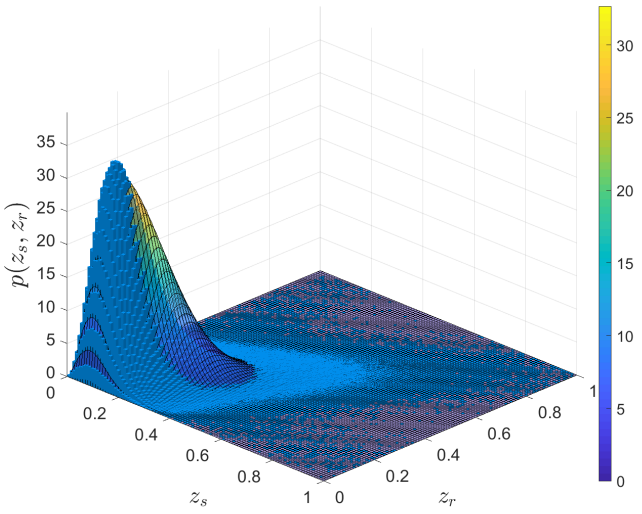

FIGURE 1. Comparison between the color-map surface plot of the theoretical Bivariate Gaussian distribution and the three-dimensional histogram obtained using empirical data from two VHF wavelength-resolution SAR difference image samples, represented by the three-dimensional blue structures.

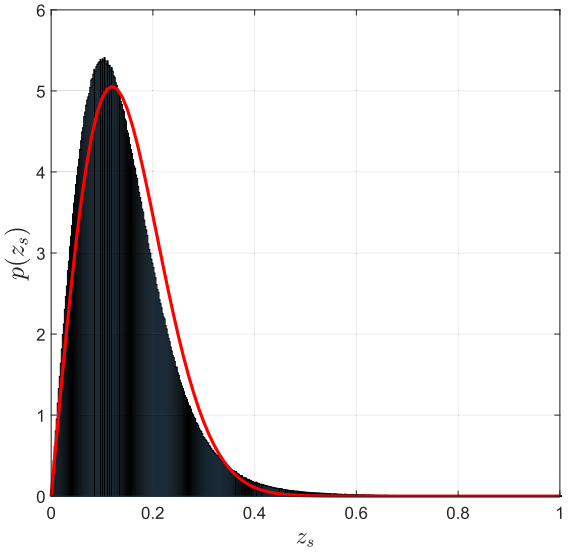

FIGURE 2. Theoretical Rayleigh distribution (curve in red) and data histogram of a VHF UWB SAR image.

observation, an application constraint was applied in [17] to mitigate the mismatch-related false alarm occurrences. The application constraint consists in setting the probability $P(s \equiv s_T | z_s, z_r) = 0$ if $z_s < z_r + \nu$, where ν is an amplitude constant. Also, this constraint enables the change detection method to detect only positive changes in the surveillance image, i.e., transforming the change detection method into a target detection method, which is frequently required for applications using VHF wavelength-resolution images [10], [11], [12], [13], [14], [15], [16], [17], [18], [19]. Finally, the necessity of an amplitude constraint shows that the model chosen for the clutter-plus-noise distribution is not ideal and justifies more investigation.

As previously mentioned in Section I, other distribution candidates were already considered for VHF wavelength-resolution SAR images, e.g., the Bivariate Gamma distribution [18] and the K-distribution [19]. However, given the heterogeneity of possible regions and structures present in SAR images, the selection of these candidate distributions may be inaccurate for different applications. This observation is also valid for the Bivariate Rayleigh distribution previously studied.

A study regarding the stability of VHF wavelength-resolution SAR images was presented in [9]. According to it, due to the characteristics of this kind of SAR image, such as their time stability, the difference images obtained from two images considering the same flight geometry can be modeled as Gaussian distributed. Thus, under similar considerations to the ones made in [18] and [19], a pair of VHF wavelength-resolution SAR difference images can be modeled as Bivariate Gaussian distributed. For the analyzes presented in this article, the difference image pairs are given by

$$z_s = z_i - z_{r2}, \tag{6}$$

$$z_r = z_{r1} - z_{r2}, \tag{7}$$

where z_i is the image of interest, which is expected to contain the targets, and z_{r1} and z_{r2} are two reference images. The Bivariate Gaussian pdf can be written as [31]

$$p(z_s, z_r) = \frac{1}{2\pi\sigma_s\sigma_r\sqrt{1-\rho^2}} \exp\left(-\frac{1}{2(1-\rho^2)}\left[\frac{(z_s-\mu_s)^2}{\sigma_s^2} + \frac{(z_r-\mu_r)^2}{\sigma_r^2} - \frac{2\rho(z_s-\mu_s)(z_r-\mu_r)}{\sigma_s\sigma_r}\right]\right), \tag{8}$$

where μ_s, μ_r, σ_s and σ_r are the mean values, and standard deviations of the difference images z_s and z_r, respectively, and ρ are the correlation coefficient that can be obtained by using (5).

Similarly to the study for the Bivariate Rayleigh distribution, Figure 3 compares the theoretical Bivariate Gaussian surface plot obtained from (8) to the three-dimensional histogram of the experimental data using a difference SAR image as an example.

As can be observed, the match between the selected Bivariate distribution and the data histogram is not ideal. Similar mismatched patterns as the ones observed for the Bivariate Rayleigh distribution are observed. Thus, similar conclusions can be drawn. However, it is possible to affirm that the Bivariate Gaussian distribution provides a better match than the Bivariate Rayleigh distribution. This better-fit results in minor mismatch regions and minor discrepancies between the probabilities values when compared with the Bivariate Rayleigh distribution. Under the same analysis made for the Rayleigh distribution, the mismatch between the data and the selected distribution is studied for a difference image under the assumption of a Gaussian distribution model. Figure 4 shows the theoretical Gaussian distribution plot and the histogram of the experimental data from the difference

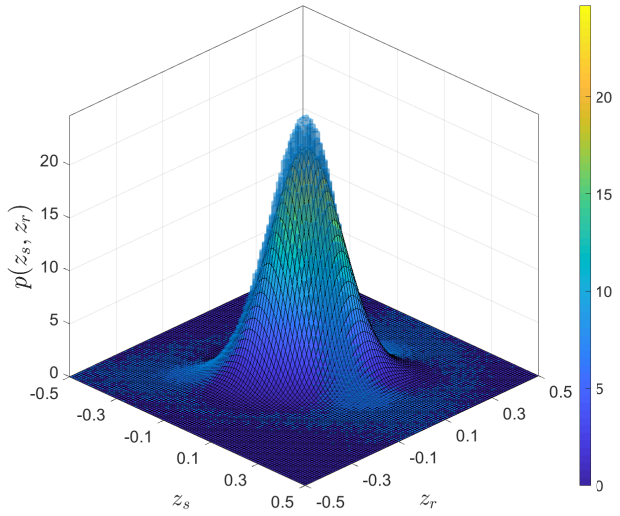

FIGURE 3. Comparison between the surface plot of the theoretical Bivariate Gaussian distribution and three-dimensional histogram obtained from a VHF wavelength-resolution SAR difference image.

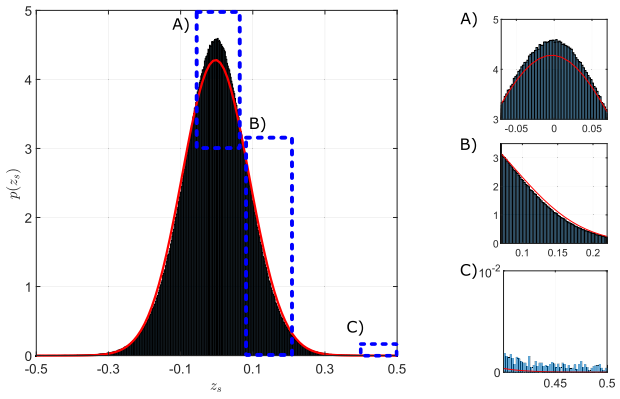

FIGURE 4. Theoretical Gaussian distribution and data histogram for a difference VHF UWB SAR image. The regions A), B), and C), where mismatches were observed, are highlighted on the right.

image. Additionally, the regions where mismatches were observed are highlighted.

Figure 4 shows three mismatch patterns. The first represented by Figure 4 A) consists of a target-like pattern occurring for small amplitudes values, i.e., $|z_s| < 0.05$. Since it is not expected that targets contain low-amplitude values, this situation tends to result in false alarm detection. However, due to the small discrepancies between the histogram and distribution model, these false alarms will only be an issue for low probability threshold values, which are very unusually selected since these thresholds tend to result in a high number of false alarms. The pattern of Figure 4 B) consists of a region where no target can be detected due to the mismatch. Due to the region's low-amplitude values, this is not an issue for the majority of the change detection applications. Finally, Figure 4 C) consists of the expected target-like pattern for adequate amplitude values. Thus, based on this analysis, there is no necessity of an amplitude constraint like the one considered for the Bivariate Rayleigh distribution.

Thus, from the presented analysis, it is possible to state that using the Bivariate Gaussian distribution for VHF wavelength-resolution SAR difference images is a better selection for the proposed iterative change detection method than using the Bivariate Rayleigh distribution. To further investigate this selection, an analysis with the Anderson-Darling (AD) GoF test considering both distributions is presented next.

A. ANDERSON-DARLING GoF EVALUATION

The Anderson Darling GoF test [32] is a nonparametric statistical test that aims to determine if a given null hypothesis would be rejected. One possible application of the AD GoF test is to investigate if a given probability distribution null hypothesis yields a good fit for an evaluated data set. The evaluation consists of performing the AD GoF test in different selected scenarios, which were chosen according to their scattering processes. For the test implementation we consider the AD GoF numerical approximation presented in [33] adopting $\alpha = 0.05$. More information regarding the AD GoF test can be found [32], [33], [34].

The evaluation presented in this paper consists of performing the AD GoF test into three different selected scenarios, which were chosen according to their scattering processes. For this evaluation, the tested data samples consist of test windows of 100×100 pixels, as considered in [10]. Figure 5 presents the three evaluation regions and the considered image samples. Finally, the evaluated regions were selected according to the following criteria.

- Region 1. - This region is characterized for not having a structure that could be defined as a dominant scatterer. Examples of this kind of scenario are open areas, lakes, and regions with small trees and bushes;
- Region 2. - This region is characterized for containing targets, i.e., vehicles;
- Region 3. - This region is characterized by having a structure that could be defined as a dominant scatterer, e.g., human-made structures such as fences, power lines, and buildings.

The AD GoF test reject the Rayleigh distribution null hypothesis for all three evaluated regions. This result was expected given the high heterogeneity of the VHF wavelength-resolution SAR images, which results in the mismatches observed in Figures 1 and 2. In contrast, the AD GoF test only rejects the Gaussian distribution null hypothesis for Region 2, i.e., it is correct to state that the Gaussian distribution is not a good option for modeling the target statistics. However, since the AD GoF test fails to reject the Gaussian distribution for Regions 1 and 3, and given that the use of difference images reduces the heterogeneity of the low-frequency wavelength-resolution SAR images, it is acceptable to assume that the Gaussian distribution provides a satisfactory statistical model for this kind of difference image.

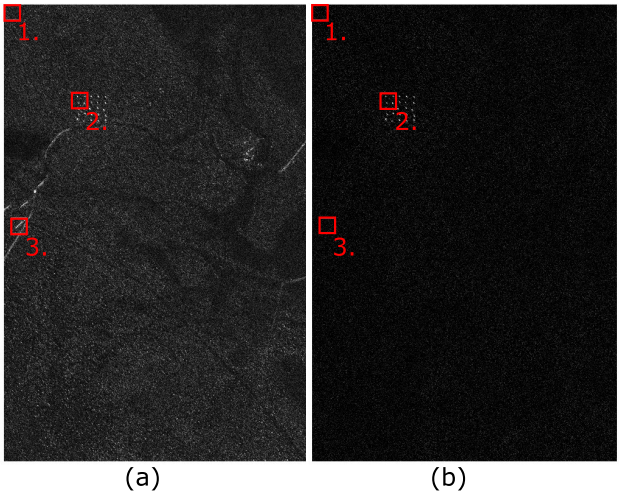

FIGURE 5. Selected scenarios for the AD GoF evaluation considering, respectively, (a) a sample image and (b) a sample difference image, where: 1) Represents an area with the absence of a strong scatterer; 2) Represents an area with a target; 3) Represents an area with the presence of a strong scatterer.

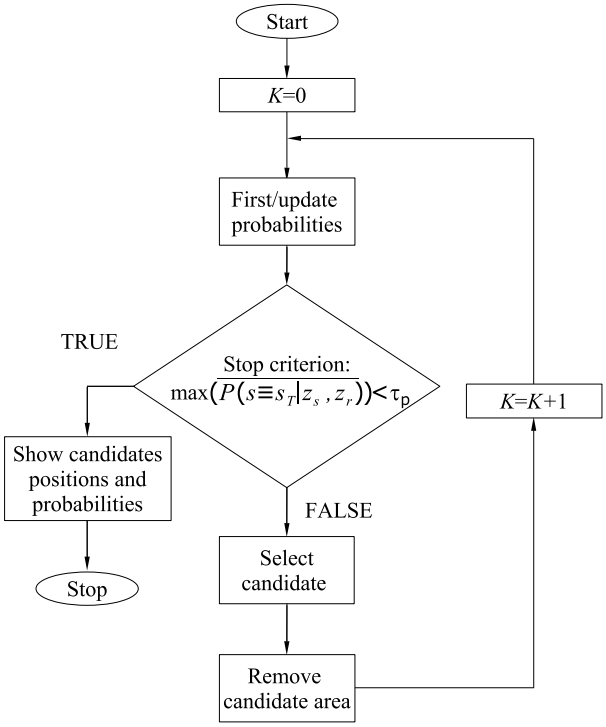

FIGURE 6. Simplified flowchart of the iterative change detection method.

IV. ITERATIVE CHANGE DETECTION METHOD

The proposed iterative change detection method is based on (3), which analyzes the mismatch between the chosen distribution and the data histogram to verify the presence of a change. A simplified flowchart for the proposed iterative method is presented in Figure 6.

The reference and surveillance images are the iterative algorithm inputs, starting with $K = 0$, where K is the number of detected targets, as previously described. The iterative approach consists of calculating the average probabilities $\overline{P(s \equiv s_T|z_s, z_r)}$ for every pixel position, selecting the pixel candidate with the highest probability to be a target if its probability is higher than a threshold probability τ_p, which lies in the range (0,1). Using average probabilities is justified to avoid selecting candidates associated with isolated pixels with unusually high probabilities. An averaging filter performs this operation with a kernel of the same size as the system resolution cell. Next, a guard area around the candidate pixel is removed. The values of the probabilities, the histogram, the parameters of the selected distribution model, and K are updated iteratively. If the pixel removal is genuinely related to a target, the parameters update tends better to match the data histogram and distribution model. Finally, the CD algorithm stops when there are no more candidates with higher average probabilities than τ_p.

Three parameters can be modified in the proposed iterative change detection, which should be selected according to the specificity of each application. The first one is the expected target size V. The second is the guard window size L, which aims to avoid same-target multiple detections. The threshold τ_p is chosen according to the desired trade-off between the probability of detection and false alarm occurrence. One example considering the selection of these parameters is presented in Section V-B.

Under the assumption that the parameters were appropriately selected for the desired application, the proposed iterative method tends to overcome the problems related to detecting isolated and multiple detections of the same target. Thus, there is no necessity to perform morphological operations, which are frequently used for such scenarios [16], [18], [24]. The output of the proposed iterative method is a set of regions centered in the selected candidate pixels. The probabilities are also available for the system operator, who can exploit the information according to the application.

An example of the correct execution of the proposed method is presented in Figure 7, considering one image from the data set employed in this study. In Figure 7, the detected targets are centered in the detected candidate pixels, highlighted by blue circles.

V. RESULTS

The data set used for the experimental evaluation is available in [6] and is presented in Section V-A. The parameters setup and other fundamental implementation aspects for the proposed method are discussed in Section V-B. Finally, performance evaluation, based on receiver operating characteristic (ROC) curves, is presented in Section V-C. A ROC curve relates the probability of detection, i.e., the ratio of the number of detected targets to the known number of targets, and false alarm rate (FAR), i.e., false alarms per square kilometer.

A. DATA DESCRIPTION

The data set comprises 24 incoherent SAR images acquired with the CARABAS II SAR system during a flight campaign in 2002, held in the military base station RFN Vidsel in

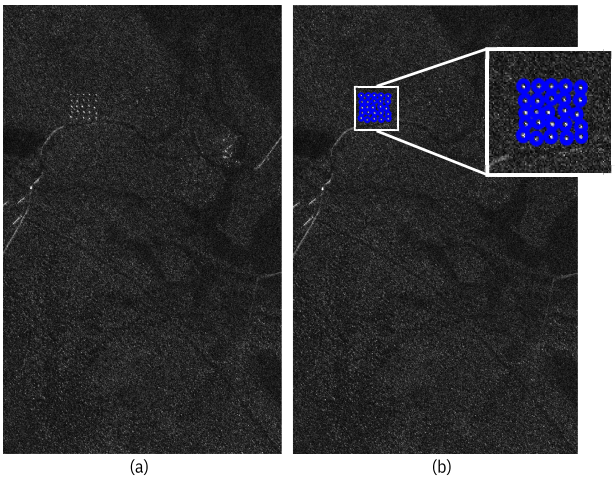

FIGURE 7. Example of detection using the proposed iterative method where (a) is the input surveillance image and (b) is the output image, where the detected targets observed in the surveillance image are in the blue circles highlighted in the image.

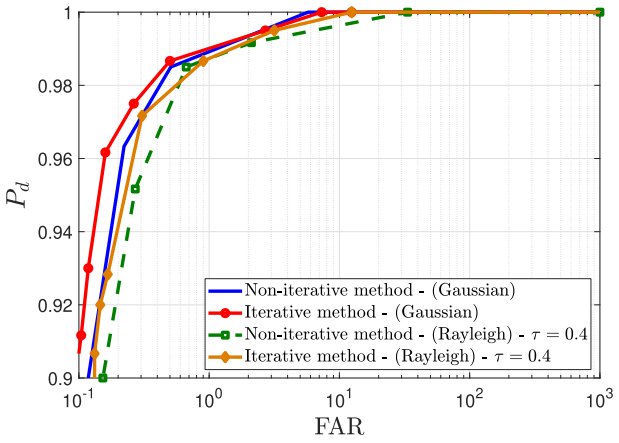

FIGURE 8. ROC performance for the proposed iterative method and the non-iterative implementation for both Rayleigh and Gaussian distributions.

northern Sweden. The region of interest is dominated by small/medium-sized trees, in which the dominant species is the Scots pine [10], but also contains lakes, roads, and fields.

Each image from the data set covers the same ground area of 6 km^2 (2 km $\times$ 3 km) and is given in the form of a 3000 $\times$ 2000 matrix. Also, each image contains 25 testing targets: ten TGB11, eight TGB30, and seven TGB40 model vehicles. The available images are already calibrated, pre-processed, and geocoded [10].

The data set images are divided into four target deployments (Missions), measured using six configurations (Passes), i.e., flight geometries. The measurements were made using the strip map SAR mode and HH polarization. Additionally, all flights were conducted with the radar looking left. More information regarding the CARABAS II data set can be found in [10] and [16].

B. IMPLEMENTATION ASPECTS

We focus on detecting targets in a surveillance image, i.e., changes associated with positive-amplitude pixels. For this scenario, the size of the expected targets is selected as $V = 30$ pixels, and a guard window L is chosen as 31×31 pixels. These selections are made based on an extrapolation of the maximum test target size and the Kernel outer size for the constant false alarm rate (CFAR) filter used in [10] and [16]. However, regarding the parameter V, it is important to highlight its influence on the probability of detecting a change since $N \gg V$ for the majority of the cases. Thus, its estimative does not require to be precise. Also, the evaluated thresholds are selected from a set of values (0, 1) to obtain the ROC curves presented in Section V-C.

For the Rayleigh distribution, the adopted constraint was the same considered in [17], where $P(s \equiv s_T | z_s, z_r) = 0$ if $z_s < z_r + \nu$. Also, similar to [17] and [18], it is adopted $\nu \in [0.2, 0.3, 0.4]$.

As stated in Section III, using Bivariate Gaussian distribution does not require amplitude constraints. However, the proposed method detects all changes present in the input images. Even knowing this scenario is helpful for some applications, detecting changes associated with negative amplitude pixels in the surveillance image is outside the desired application and would grant an unfair comparison with other methods using the same data set. To guarantee the detection of only targets related to positive changes in the surveillance image, the following constraint is applied $P(s \equiv s_T | z_s, z_r) = 0$ if $z_s < 0$ or $z_s < z_r$.

C. EXPERIMENTAL RESULTS

We first verified if the proposed iterative CD method excels the non-iterative method proposed in [17]. Figure 8 presents the ROC curves of both evaluated schemes. For better visualization, it only showed the ROC curves for $\tau = 0.4$ since it granted the best performance.

The results presented in Figure 8 shows that the iterative method outperforms the non-iterative techniques for most of the evaluated points. For instance, the evaluated points with $P_d = 0.95$ are associated with the following false alarm rates: FAR ≈ 0.143 for the iterative method using the Bivariate Gaussian distribution, whereas FAR ≈ 0.1944 is observed for the non-iterative case; FAR ≈ 0.2255 for the iterative technique using the Bivariate Rayleigh distribution, whereas FAR ≈ 0.2658 is kept for the non-iterative case; This observed pattern is expected for scenarios with low false alarms. In these scenarios, most information provided for updating the distribution/histogram is accurate, translating into better performance. However, in high false alarm scenarios, wrong information could be used to update the statistics decreasing the method's performance. Moreover, the performance of both iterative/non-iterative methods using the Bivariate Gaussian distribution overcomes those using the Bivariate Rayleigh distribution.

The second comparison was between the proposed iterative CD method and five CD techniques presented

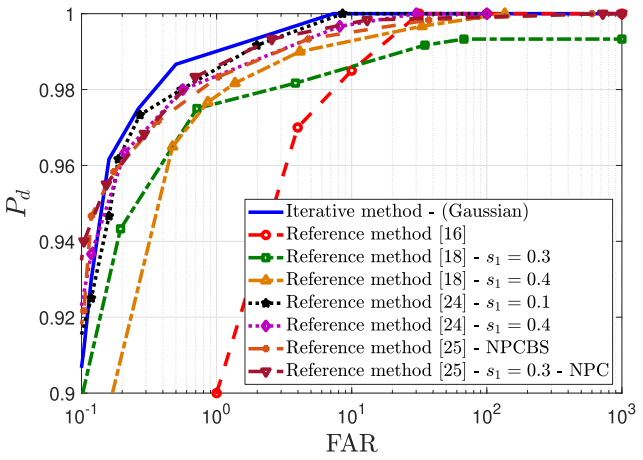

FIGURE 9. ROC performance for the proposed iterative method, using the Bivariate Gaussian distribution, and for the reference methods [16], [18], and [24], and [25].

in [16], [18], [24], and [25]. The technique presented in [16] was one of the first methods to perform change detection in CARABAS II images. The method proposed in [18] provides one of the best performances for the CARABAS II data set, using only an image pair as input. The method proposed in [24] uses three SAR images as input. To the best of the author's knowledge, the technique presented in [24] has one of the best performances in terms of FAR and P_d for the evaluated data set. Finally, the two methods proposed in [25], named Change Detection Method Based on NP Using only Background Statistics (NPCBS) and Change Detection Method Based on NP-Criterion (NPC), are CD methods that consider the use of SAR image stacks, with no target statistics information or small knowledge regarding target statistics, respectively. Both NPCBS and NPC methods obtained competitive performance in terms of the evaluated metrics for the considered data set when compared with updated change detection methods from the literature. Figure 9 illustrates the performance of the proposed method and the best ROC curves presented in [16], [18], [24], and [25].

The proposed iterative method outperforms all other techniques for most of the tested points. Considering the points with FAR = 10^0, the proposed iterative approach achieves the performance of $P_d \approx 0.99$. For the same evaluated point, the method presented in [16] has $P_d \approx 0.90$; the technique shown in [18] has $P_d \approx 0.978$ and $P_d \approx 0.976$ for $s_1 = 0.3$ and 0.4, respectively, where s_1 is an amplitude constraint. Reference [24] achieves $P_d \approx 0.9854$ and $P_d \approx 0.9836$ for $s_1 = 0.4$ and $s_1 = 0.1$, respectively. The methods presented in [25] achieve $P_d \approx 0.9830$ and $P_d \approx 0.9861$ for NPCBS and the NPC methods, respectively.

VI. DISCUSSION

The performance of the proposed iterative change detection method was assessed by ROC curves in Figures 8 and 9. As can be seen, the proposed method outperforms the other evaluated methods. Moreover, using difference images as input allowed a simpler distribution model, i.e., the Bivariate Gaussian distribution. This solution reduces the necessity of computational resources and processing time.

Finally, as discussed in Section IV, the proposed method can detect positive and negative changes, allowing for other applications besides target detection in forestry areas. Evaluating the proposed method for different applications and data sets may be explored in future studies.

VII. FINAL REMARKS

This paper proposed an iterative CD method based on Bayes' theorem for wavelength-resolution VHF SAR images using traditional clutter-plus-noise statistical models. The proposed approach uses the information of the detected changes to iteratively update the data and distribution statistics, obtaining more accurate information and, consequently, reducing false alarms.

Aiming to emphasize the dependency of the proposed iterative CD method on the clutter-plus-noise model, we considered two distributions as candidates, namely Bivariate Rayleigh and Bivariate Gaussian distributions. The analysis was made using the AD GoF test. We conclude that the Bivariate Gaussian distribution is a good candidate for modeling the clutter-plus-noise of difference VHF wavelength-resolution SAR images, yielding a good match for the evaluated data set.

The results showed that the proposed method presented a competitive performance compared to state-of-the-art CD methods for VHF UWB SAR images. In this work, we only considered two well-known distributions as candidates to model the clutter-plus-noise. Investigating other distributions to model the clutter-plus-noise statistics could grant additional performance gains, an interesting topic for future research.

REFERENCES

[1] M. Kirscht, J. Mietzner, B. Bickert, A. Dallinger, J. Hippler, J. Meyer-Hilberg, R. Zahn, and J. Boukamp, "An airborne radar sensor for maritime and ground surveillance and reconnaissance—Algorithmic issues and exemplary results," *IEEE J. Sel. Topics Appl. Earth Observ. Remote Sens.*, vol. 9, no. 3, pp. 971–979, Mar. 2016.

[2] Y. Wang, Z. Zhang, N. Li, F. Hong, H. Fan, and X. Wang, "Maritime surveillance with undersampled SAR," *IEEE Geosci. Remote Sens. Lett.*, vol. 14, no. 8, pp. 1423–1427, Aug. 2017.

[3] B. Snapir, T. W. Waine, R. Corstanje, S. Redfern, J. De Silva, and C. Kirui, "Harvest monitoring of Kenyan tea plantations with X-band SAR," *IEEE J. Sel. Topics Appl. Earth Observ. Remote Sens.*, vol. 11, no. 3, pp. 930–938, Mar. 2018.

[4] W. Melvin and J. Scheer, *Principles of Modern Radar: Radar Applications*, vol. 3, 1st ed. Rijeka, Croatia: SciTech, 2014.

[5] H. Hellsten, L. M. H. Ulander, A. Gustavsson, and B. Larsson, "Development of VHF CARABAS II SAR," *Proc. SPIE*, vol. 2747, pp. 48–60, Jun. 1996.

[6] U.S. Air Force. *The Sensor Data Management System—SDMS*. Accessed: Mar. 26, 2018. [Online]. Available: https://www.sdms.afrl.af.mil/

[7] L. Ulander, "VHF-band SAR for detection of concealed ground targets," in *Proc. RTO SCI Symp. Sensors Sensor Denial Camouflage, Concealment Deception*, Apr. 2004, pp. 19-1–19-11.

[8] G. Smith and L. M. H. Ulander, "A model relating VHF-band backscatter to stem volume of coniferous boreal forest," *IEEE Trans. Geosci. Remote Sens.*, vol. 38, no. 2, pp. 728–740, Mar. 2000.
[9] R. Machado, V. T. Vu, M. I. Pettersson, P. Dammert, and H. Hellsten, "The stability of UWB low-frequency SAR images," *IEEE Geosci. Remote Sens. Lett.*, vol. 13, no. 8, pp. 1114–1118, Aug. 2016.
[10] M. Lundberg, L. M. H. Ulander, W. E. Pierson, and A. Gustavsson, "A challenge problem for detection of targets in foliage," *Proc. SPIE*, vol. 6237, pp. 160–171, May 2006.
[11] Y. Sun, L. Lei, D. Guan, G. Kuang, and L. Liu, "Graph signal processing for heterogeneous change detection," *IEEE Trans. Geosci. Remote Sens.*, vol. 60, 2022, Art. no. 4415823.
[12] Y. Sun, L. Lei, X. Li, X. Tan, and G. Kuang, "Structure consistency-based graph for unsupervised change detection with homogeneous and heterogeneous remote sensing images," *IEEE Trans. Geosci. Remote Sens.*, vol. 60, 2022, Art. no. 4700221.
[13] J. G. Vinholi, D. Silva, R. Machado, and M. I. Pettersson, "CNN-based change detection algorithm for wavelength-resolution SAR images," *IEEE Geosci. Remote Sens. Lett.*, vol. 19, pp. 1–5, 2022.
[14] A. B. Campos, M. I. Pettersson, V. T. Vu, and R. Machado, "False alarm reduction in Wavelength–Resolution SAR change detection schemes by using a convolutional neural network," *IEEE Geosci. Remote Sens. Lett.*, vol. 19, pp. 1–5, 2022.
[15] Z. Liu, Z. Chen, and L. Li, "An automatic high confidence sets selection strategy for SAR images change detection," *IEEE Geosci. Remote Sens. Lett.*, vol. 19, pp. 1–5, 2022.
[16] L. M. H. Ulander, M. Lundberg, W. Pierson, and A. Gustavsson, "Change detection for low-frequency SAR ground surveillance," *IEE Proc.-Radar, Sonar Navigat.*, vol. 152, no. 6, pp. 413–420, Dec. 2005.
[17] D. I. Alves, B. G. Palm, H. Hellsten, V. T. Vu, M. I. Pettersson, R. Machado, B. F. Uchôa-Filho, and P. Dammert, "Wavelength-resolution SAR change detection using Bayes' theorem," *IEEE J. Sel. Topics Appl. Earth Observ. Remote Sens.*, vol. 13, pp. 5560–5568, Sep. 2020.
[18] V. T. Vu, N. R. Gomes, M. I. Pettersson, P. Dammert, and H. Hellsten, "Bivariate gamma distribution for wavelength-resolution SAR change detection," *IEEE Trans. Geosci. Remote Sens.*, vol. 57, no. 1, pp. 473–481, Jan. 2019.
[19] N. R. Gomes, P. Dammert, M. I. Pettersson, V. T. Vu, and H. Hellsten, "Comparison of the Rayleigh and K-distributions for application in incoherent change detection," *IEEE Geosci. Remote Sens. Lett.*, vol. 16, no. 5, pp. 756–760, May 2019.
[20] D. I. Alves, B. G. Palm, M. I. Pettersson, V. T. Vu, R. Machado, B. F. Uchôa-Filho, P. Dammert, and H. Hellsten, "A statistical analysis for wavelength-resolution SAR image stacks," *IEEE Geosci. Remote Sens. Lett.*, vol. 17, no. 2, pp. 227–231, Feb. 2020.
[21] Z. Xu, "Wavelength-resolution SAR speckle model," *IEEE Geosci. Remote Sens. Lett.*, vol. 19, pp. 1–5, 2022.
[22] H. Hellsten, R. Machado, M. I. Pettersson, V. T. Vu, and P. Dammert, "Experimental results on change detection based on Bayes probability theorem," in *Proc. IEEE Int. Geosci. Remote Sens. Symp. (IGARSS)*, Jul. 2015, pp. 318–321.
[23] H. Hellsten and R. Machado, "Bayesian change analysis for finding vehicle size targets in VHF foliage penetration SAR data," in *Proc. IEEE Radar Conf.*, Oct. 2015, pp. 510–515.
[24] V. T. Vu, "Wavelength-resolution SAR incoherent change detection based on image stack," *IEEE Geosci. Remote Sens. Lett.*, vol. 14, no. 7, pp. 1012–1016, Jul. 2017.
[25] D. I. Alves, C. Müller, B. G. Palm, M. I. Pettersson, V. T. Vu, R. Machado, B. F. Uchôa-Filho, P. Dammert, and H. Hellsten, "Neyman–Pearson criterion-based change detection methods for Wavelength–Resolution SAR image stacks," *IEEE Geosci. Remote Sens. Lett.*, vol. 19, pp. 1–5, 2022.
[26] M. Zhao, Q. Ling, and F. Li, "An iterative feedback-based change detection algorithm for flood mapping in SAR images," *IEEE Geosci. Remote Sens. Lett.*, vol. 16, no. 2, pp. 231–235, Feb. 2019.
[27] Q. Yu, M. Zhang, L. Yu, R. Wang, and J. Xiao, "SAR image change detection based on joint dictionary learning with iterative adaptive threshold optimization," *IEEE J. Sel. Topics Appl. Earth Observ. Remote Sens.*, vol. 15, pp. 5234–5249, 2022.
[28] Y. Sun, L. Lei, D. Guan, and G. Kuang, "Iterative robust graph for unsupervised change detection of heterogeneous remote sensing images," *IEEE Trans. Image Process.*, vol. 30, pp. 6277–6291, 2021.
[29] N. R. Gomes, M. I. Pettersson, V. T. Vu, P. Dammert, and H. Hellsten, "Likelihood ratio test for incoherent wavelength-resolution SAR change detection," in *Proc. CIE Int. Conf. Radar (RADAR)*, Oct. 2016, pp. 1–4.
[30] M. K. Simon and M.-S. Alouini, "A simple single integral representation of the bivariate Rayleigh distribution," *IEEE Commun. Lett.*, vol. 2, no. 5, pp. 128–130, May 1998.
[31] A. Papoulis, *Probability, Random Variables, and Stochastic Processes*, 4th ed. Boston, MA, USA: McGraw-Hill, 2002.
[32] T. W. Anderson and D. A. Darling, "Asymptotic theory of certain 'goodness of fit' criteria based on stochastic processes," *Ann. Math. Statist.*, vol. 23, no. 2, pp. 193–212, Jun. 1952.
[33] G. Marsaglia and J. Marsaglia, "Evaluating the anderson-darling distribution," *J. Stat. Softw.*, vol. 9, no. 2, pp. 1–5, 2004.
[34] H. Wang, E.-H. Yang, Z. Zhao, and W. Zhang, "Spectrum sensing in cognitive radio using goodness of fit testing," *IEEE Trans. Wireless Commun.*, vol. 8, no. 11, pp. 5427–5430, Nov. 2009.

DIMAS IRION ALVES (Member, IEEE) received the B.S.E.E. degree from the Federal University of Santa Maria (UFSM), Santa Maria, Rio Grande do Sul, Brazil, in 2013, and the M.Sc. and Ph.D. degrees in electrical engineering from the Federal University of Santa Catarina (UFSC), Florianópolis, Santa Catarina, Brazil, in 2015 and 2020, respectively. From 2018 to 2019, he was a Visiting Ph.D. Researcher Fellow with the Blekinge Institute of Technology (BTH), Sweden. From 2015 to 2021, he was a Professor with the Federal University of Pampa (Unipampa), Alegrete, Rio Grande do Sul. Since September 2021, he has been a Professor with the Department of Telecommunications, Aeronautics Institute of Technology (ITA), and the Graduate Program in Electronics and Computer Engineering (PG/EEC), ITA, São José dos Campos, São Paulo, Brazil. His current research interests include radars, SAR systems, image processing, and digital signal processing.

BRUNA GREGORY PALM (Member, IEEE) received the B.Sc. degree in statistics from the Federal University of Santa Maria (UFSM), Santa Maria, Brazil, in 2014, and the D.Sc. degree in statistics from the Federal University of Pernambuco (UFPE), Recife, Brazil, in 2020. From February 2018 to January 2019, she was a Guest Ph.D. Researcher with the Blekinge Institute of Technology (BTH), Karlskrona, Sweden. From April 2020 to March 2021, she was a Research Fellow with the Department of Telecommunications, Aeronautics Institute of Technology (ITA), São José dos Campos, Brazil. From August 2021 to November 2021, she was a Visiting Research Fellow with BTH in partnership with Saab AB. She is currently an Associate Senior Lecturer with BTH. Her current research interests include data science, regression/dynamic models, statistical computing, parametric inference, SAR data, and statistical signal/image processing. Her doctoral dissertation received the Commission Outstanding Award from the Brazilian Society of Applied and Computational Mathematics, Brazil, in 2021.

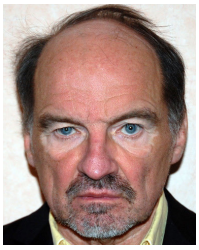

HANS HELLSTEN (Senior Member, IEEE) received the Ph.D. degree in theoretical physics from the University of Stockholm, Stockholm, Sweden, in 1981. His basic expertise is as a theoretical physics doctor. He started radar research with the Swedish Defense Research Agency FOI, subsequently appointed as the Research Director, where he directed the development of new methods for meter-wave synthetic aperture radar, since 1986. The work soon acquired significant national and international interest and a major Swedish foliage penetration meter-wave SAR research program was formed. Amongst various achievements, the airborne CARABAS I and II radars were produced. In 2001, he was the Principal Engineer of meter-wave radar development with Ericsson Microwave Systems (nowadays, Saab Surveillance). He there directed the development of foliage penetration radar system modeling and optimization run in parallel with experimental verification with the CARABAS III radar system built for this purpose. In a joint Halmstad/Saab research effort, he is currently developing new methods for suppressing mutual interference between radars and between radar and communication. He is currently a Senior Radar Expert with Saab and an Adjunct Professor of radar systems with Halmstad University. His work has led to a large number of patents and scientific publications and has rendered him the Polhem Prize for technological innovation, the Gold Medal for outstanding engineering work from the Royal Swedish Academy of Engineering Sciences (IVA), and the Thulin Medal for aerospace technology achievements. Recently, he made a cohesive account of foliage penetration technology and physics in the form of the book *Meter-Wave Synthetic Aperture Radar for Concealed Object Detection* (Artech House Publishers).

RENATO MACHADO (Senior Member, IEEE) was born in Jaú, São Paulo, Brazil, in 1979. He received the B.S.E.E. degree from São Paulo State University (UNESP), Ilha Solteira, São Paulo, in 2001, and the master's and Ph.D. degrees in electrical engineering from the Federal University of Santa Catarina (UFSC), Florianópolis, Santa Catarina, Brazil, in 2004 and 2008, respectively. He was a Visiting Ph.D. Scholar with the Department of Electrical Engineering, Arizona State University (ASU), Tempe, AZ, USA, from August 2006 to June 2007. From November 2013 to February 2015, he was a Visiting Research Fellow with the Blekinge Institute of Technology (BTH), Karlskrona, Sweden, in partnership with Saab AB, Sweden. From August 2009 to December 2017, he was with the Federal University of Santa Maria, Rio Grande do Sul, Brazil, where he was an Assistant Professor, from 2008 to 2016, an Associate Professor, in 2017, and lectured many courses in bachelor's and graduate programs and assumed different positions in the institution, namely, the Research Leader of the Communications and Signal Processing Research Group, the Coordinator of the Telecommunications Engineering Program, and the Director of the Aerospace Science Laboratory. Since December 2017, he has been an Associate Professor with the Aeronautics Institute of Technology (ITA), São José dos Campos, São Paulo. He is also the Research Leader of the Digital and Signal Processing Laboratory and the SAR and Radar Signal Processing Laboratory, ITA. His current research interests include synthetic aperture radar (SAR) processing, SAR image processing, change detection, radar signal processing, wireless communications, and digital signal processing.

VIET THUY VU (Senior Member, IEEE) received the Ph.D. degree in applied signal processing from the Blekinge Institute of Technology (BTH), Karlskrona, Sweden, in 2011. Since 2013, he has been with the Department of Mathematics and Natural Science, BTH, where he has been a Post-Doctoral Researcher of radar algorithm development, an Assistant Professor of radar remote sensing, and currently an Associate Professor of system engineering. He has authored or coauthored more than 100 scientific publications. His current research interests include SAR signal processing, applications of SAR in change detection and SAR GMTI, and radio occultation.

MATS I. PETTERSSON (Senior Member, IEEE) received the M.Sc. degree in engineering physics, the Licentiate degree in radio and space science, and the Ph.D. degree in signal processing from the Chalmers University of Technology, Gothenburg, Sweden, in 1993, 1995, and 2000, respectively. He was with the Mobile Communication Research, Ericsson, Lund, Sweden. He was with the Swedish Defense Research Agency (FOI), Linkping, Sweden, for ten years. At FOI, he focused on ultrawideband low-frequency SAR systems. Since 2005, he has been with the Blekinge Institute of Technology (BTH), Karlskrona, Sweden, where he is currently a Full Professor. He has authored or coauthored more than 200 scientific publications, of which more than 60 are in peer-reviewed scientific journals. His current research interests include radar surveillance, remote sensing, SAR processing, space-time adaptive processing (STAP), high-resolution SAR change detection, automotive radar, radio occultation, THz SAR, and computer vision.

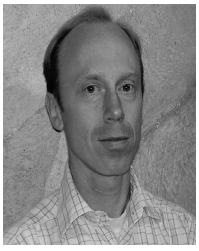

PATRIK DAMMERT (Senior Member, IEEE) received the M.Sc. degree in electrical engineering and the Ph.D. degree in spaceborne SAR interferometry from the Chalmers University of Technology, Gothenburg, Sweden, in 1993 and 1999, respectively. He joined Saab, in 2000, and started to work with demonstrators for SAR and GMTI radar technologies. Later, he led or co-led the research and development of high-performance SAR and GMTI systems, spanning from VHF-band to X-band radar systems. He has been involved in or initiated or led many research collaboration projects (starting around 2004) with the Chalmers University of Technology, Purdue University, Aalto University, and the Blekinge Institute of Technology. In 2015, he was appointed a Specialist of signal processing algorithms with Saab. Since 2019, he has been an Adjunct Professor with the Chalmers University of Technology, with an emphasis on signal processing for radar systems. His current research interests include algorithms and signal processing for high-performance radar, bistatic and multi-static radar, SAR autofocus, and target detection in complicated radar clutter.